Modelling and Simulation of the CLS Cryogenic System

C. Veeramani[1,*], R. J. Spiteri[1]

Department of Computer Science, University of Saskatchewan, 176 Thorvaldson Building, 110 Science Place, Saskatoon, SK S7N 5C9, Canada.

Abstract

This paper presents results pertaining to the numerical modelling of the cryogenic system at the Canadian Light Source. The cryogenic system consists of a cryostat that houses a Radio Frequency (RF) cavity used for boosting the energy of an electron beam. For consistent operation of the RF cavity, it must be kept immersed in liquid helium at a constant level with the pressure in the gas space maintained to an accuracy of ± 1 mbar. An improvement to the cryostat model suggested in [1] using control volumes is described. The model and numerical method developed for the liquid helium supply and gaseous helium return lines are validated using two different cases, viz., the liquid helium flow rate from the liquid helium transfer line and the gaseous helium flow rate from the cryostat for various heater power input settings. The numerical method described here is significantly more accurate, efficient, and flexible than that used in [2] based on an iterative bisection method.

Keywords: Cryogenics, helium, two-phase flow, process modelling

1. Introduction

The Canadian Light Source (CLS) is a unique research facility in Canada that produces extremely bright light in a synchrotron. The electron beam used for this purpose loses energy with every photon emitted, but the beam is re-energized in a Radio Frequency (RF) cavity made of niobium that is maintained in a superconducting state using liquid helium at 4.5 K. Maintaining this low temperature requires accurate control of the pressure and

*Corresponding author.

Email addresses: c.veeramani@usask.ca (C. Veeramani), spiteri@cs.usask.ca (R. J. Spiteri)

level of liquid helium in the cryostat in which the RF cavity is housed. We wish to numerically model the process equipment that makes up the cryogenic system in order to gauge the sensitivity of the pressure and level of liquid helium to changes in the control valve opening. In this report, we present the mathematical formulation and results of dynamic simulations of the cryostat in the cryogenic system using a control-volumes approach.

1.1. The process description

As depicted in Figure 1, gaseous helium (GHe) is compressed and cooled to 10 K by compressors and turbines with heat exchangers. Further cooling is achieved through the Joule–Thomson effect by expansion through a valve. Liquid helium (LHe) is collected in a vessel called a *dewar*, which has a capacity of 2000 L. The pressure and liquid level in the dewar are maintained by standard proportional-integral (PI) controllers. The pressure controller returns cold GHe through the heat exchangers. The normal operating pressure in the dewar is 1.37 bars, corresponding to a saturation temperature of 4.5 K; however it may vary between 1.35 bars and 1.38 bars. The liquid level in the dewar is maintained using resistor heating, which activates if the level is too high. This resistor and the Joule–Thomson valve position are used together with a level and a pressure transmitter to maintain the LHe level and pressure in the dewar.

The RF cavity is housed inside the cryostat, which is equipped with a level controller and a pressure controller. Similar to the situation in the dewar, the pressure controller maintains a set pressure by returning cold GHe to the heat exchangers. The normal operating pressure in the cryostat is 1.22 bars, corresponding to a saturation temperature of 4.4 K; however it may vary between 1.19 bars and 1.23 bars. The LHe delivered from the dewar to the cryostat is expected to boil off in the cryostat, thus cooling the LHe in the cryostat. There is power dissipation into the cryostat from three sources, namely, the RF cavity, the heating resistor that is used to maintain the liquid level, and static heat loading into the system through various instruments. The liquid level is regulated by a control valve on the LHe transfer line from the dewar. Another GHe line is drawn from the cryostat to keep the waveguide cold. The waveguide is the energy transfer device to the RF cavity that must be protected from thermal shock because part of it is inside the cryostat and part is at room temperature ($\sim$300 K). Further, a liquid nitrogen line is also used in cooling the waveguide. The GHe drawn from the cryostat is at a set flow rate of 25 L/min, controlled by

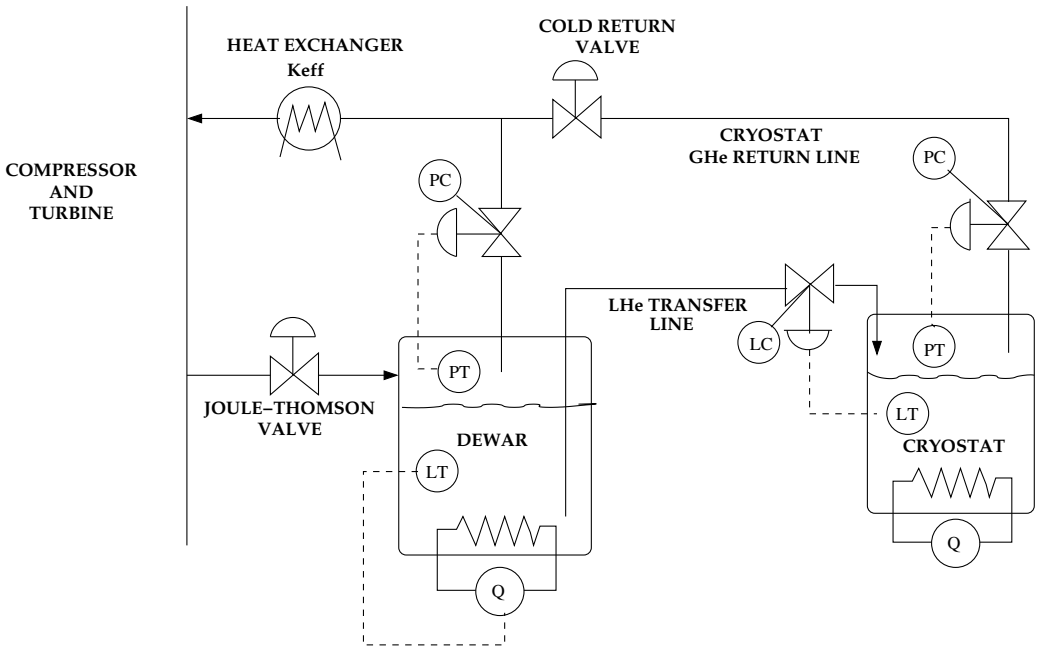

Figure 1: The part of the process flow of the cryogenic system modeled.

a flow controller. Note that this flow rate is measured at room temperature; at the conditions in the cryostat, the flow is negligible (0.2% of the overall flow through the cryostat).

1.2. Outline of this report

The operation of the cryostat must be at a consistent set pressure for the RF cavity to produce an electron beam of consistent energy. Chattering of control valves or formation of two phases in the LHe transfer line can cause unacceptably large pressure fluctuations in the cryostat. The motivation for this work is to mathematically model and numerically simulate the cryogenic system in order to understand the source(s) of pressure fluctuations in the transfer line, potentially due to two-phase formation or sensitivity of the system to control-valve operations. This could lead to various levels of process modification. Near-term modifications may include changing the operating conditions or the control valves and their operation method, e.g., pneumatically operated or electrically motorized operation. In the long term, the effects of dramatic process changes such as

- shortening the length of transfer line by moving the dewar closer to the cryostat
- adding a standby set of dewar and cryostat to avoid shutdown

could be studied based on this work.

A one-dimensional homogeneous flow model coupled with thermodynamic properties model for helium has been developed in [2]. The computational approach was based on an iterative bisection method used for solving one-dimensional homogeneous flow model. This work presents a more efficient, accurate, and flexible computational approach based on control-volume balances for steady-state flow to predict the void fraction, velocity, and liquid flow rate in the transfer line. A similar approach is adapted to predict the pressure, temperature, and velocity in the gas return line.

The pipe network currently modeled includes the LHe transfer line from the dewar to the cryostat and the GHe return lines, namely, the GHe return from the cryostat to the T-junction, the GHe return from the dewar to the T-junction, and the combined GHe line after the T-junction across the heat exchangers up to the suction of compressors; see Figure 1. The LHe line has a level control valve (LCV) that is regulated by a PI controller based on the signal from the level transmitter in the cryostat. The GHe return line has a pressure control valve (PCV) that is regulated by a PI controller based on the signal from the pressure transmitter in the cryostat and a cold return valve (CRV) that diverts flow to heat exchanger if the temperature of the GHe is below a certain set limit; otherwise the GHe passes through the warm return valve (not shown) for further cooling. The specifications for the various sections of the LHe line from the dewar to the cryostat and the GHe network are presented in [3]. A detailed account of the cross-sectional geometry of the pipe is also discussed there. The heat loading on the LHe transfer line and the GHe return line is of special importance and is discussed in [3]. The lumped system model based on a control-volumes approach is discussed in Section 2 for the LHe transfer line and in Section 3 for the GHe return line. Unlike the pipes, which are modeled as stationary lumped systems, the cryostat in which the RF cavity is housed is modeled as a dynamic system in order to capture the fluctuations in pressure and level. The details of the cryostat model are discussed in Section 4. The model equations, their implementation, and the numerical schemes employed to simulate the cryostat along with the controllers, liquid supply line, and gas return line are discussed in Section 5. The results of the lumped system model and the

one-dimensional homogeneous model are compared in Section 6. We discuss two validation cases: one for the liquid flow rate from the LHe transfer line and another for the dynamics of cryostat operation along with heater input and PCV and LCV operation in addition to the LHe supply and GHe return flow rates. Finally, the key contributions are listed in Section 7.

2. Two-Phase Flow Model

The model proposed in [1] is a one-dimensional homogeneous-phase model for the two-phase liquid-gas flow in the transfer line. The model is one dimensional in that it ignores variation in properties in the radial and azimuthal directions. Further, it is assumed that the gas phase fraction (or void fraction, α) is less than 0.2, corresponding to bubbly flow throughout the pipe. The flow is also assumed to be turbulent; thus the flow is effective in mixing the gas and liquid phases. The model consists of equations for the conservation of gas mass, liquid mass, overall homogeneous phase momentum, and overall homogeneous phase energy balance [2].

The entire liquid transfer line can be considered as one control volume. The fluid enters the control volume as saturated liquid ($\alpha_{in} = 0$). The fluid is assumed to flash in the control volume. In the real LHe transfer line, the liquid flashes due to a reduction in pressure from line losses and from heat transferred into the line through conduction and radiation. If the control volume is considered adiabatic, then the reduction in pressure means the boiling point of the fluid is reduced. When the boiling point reaches the liquid temperature, the liquid flashes.

Given the inlet and outlet pressures and the void fraction of the fluid entering the control volume, we are interested in estimating the void fraction at the outlet (α_{out}) and the velocities at the inlet (v_{in}) and the outlet (v_{out}). We solve for these three variables from the conservation equations for mass, momentum, and energy. However, in order to capture the dynamics associated with the opening and closing of the control valve and the pressure losses at each pipe fitting and line segment, the LHe transfer line is subdivided into multiple control volumes, with end points placed where process variables are to be evaluated; more details are given in Section 5. The remainder of this section outlines the governing equations as applied to a single control volume.

2.1. Mass balance for two-phase flow system

The mass balance equation for a control volume can be written as [4]:

$$\frac{\mathrm{d}m_{tot}}{\mathrm{d}t} = \mathcal{F}_{in} - \mathcal{F}_{out} + r_{gen},$$

where m_{tot} is the total mass in the control volume, $\mathcal{F}_{in}$ and $\mathcal{F}_{out}$ are the rates of mass flow into and out of the control volume, and r_{gen} is the rate of generation of mass. For our application, when considering the overall mass balance in a control volume, there is no generation of mass inside the volume. However, this equation can be split into mass balance equations for the two phases separately, taking into account the mass transferred between the phases, to yield

$$\frac{\mathrm{d}m_g}{\mathrm{d}t} = \mathcal{F}_{g,in} - \mathcal{F}_{g,out} + r_{boil}$$

and

$$\frac{\mathrm{d}m_l}{\mathrm{d}t} = \mathcal{F}_{l,in} - \mathcal{F}_{l,out} - r_{boil},$$

where the subscript g denotes the gas phase and l denotes the liquid phase. The term r_{boil} denotes the rate at which mass is transferred from the liquid phase to the gas phase. This term can be further related to the rate of heat used in vaporization $\dot{Q}_{boil}$ and the latent heat of vaporization ζ as

$$r_{boil} = \frac{\dot{Q}_{boil}}{\zeta}. \tag{1}$$

At steady state, the conservation of total mass gives

$$0 = \mathcal{F}_{in} - \mathcal{F}_{out}. \tag{2}$$

In terms of void fraction α, phase densities ρ_g and ρ_l, overall homogeneous velocities v, and cross-sectional areas A, this reduces to

$$\underbrace{(\rho_{g,in}\alpha_{in} + \rho_{l,in}(1-\alpha_{in}))}_{\rho_{in}} A_{in}v_{in} = \underbrace{(\rho_{g,out}\alpha_{out} + \rho_{l,out}(1-\alpha_{out}))}_{\rho_{out}} A_{out}v_{out}, \tag{3}$$

where the density of the fluid at the inlet ρ_{in} is given in terms of the void fraction as $(\rho_{g,in}\alpha_{in} + \rho_{l,in}(1-\alpha_{in}))$ and similarly the density at the outlet of the control volume ρ_{out} is given in terms of the void fraction as $(\rho_{g,out}\alpha_{out} + \rho_{l,out}(1-\alpha_{out}))$.

2.2. Momentum balance for two-phase flow system

The momentum balance for a control volume [4] can be written for one-dimensional flow as

$$\begin{aligned}\frac{\mathrm{d}p_{tot}}{\mathrm{d}t} &= (P_{in}A_{in} - P_{out}A_{out}) + m_{tot}g\sin\theta \\ &\quad - F_f + \left(\rho_{in}v_{in}^2A_{in} - \rho_{out}v_{out}^2A_{out}\right),\end{aligned}$$

where P_{in} and P_{out} are the pressures, A_{in} and A_{out} are the cross-sectional areas, g is the acceleration due to gravity, θ is the angle that the pipe makes with the horizontal, and F_f represents the net force on the fluid due to solid boundaries. The quantities ρ_{in}, ρ_{out} are calculated from (3). If the inlet and outlet areas are equal, i.e., $A_{in} = A_{out} \equiv A = \frac{\pi}{4}d^2$, where d is the diameter of the pipe, then the total mass in the control volume can be written as $\langle\rho\rangle AL$, where L is the length of the pipe and $\langle\rho\rangle = (\rho_{in}+\rho_{out})/2$ is an approximation to the average fluid density. Further, the change in elevation of the ends of the control volume can be written as $L\sin\theta = \Delta z$. The momentum balance for steady-state conditions, after dividing by A, can be written as

$$0 = (P_{in} - P_{out}) + \langle\rho\rangle\,(g\Delta z) - \frac{1}{2}\langle\rho\rangle\langle v\rangle^2\left(\frac{L}{d}f_f + K\right) + \left(\rho_{in}v_{in}^2 - \rho_{out}v_{out}^2\right), \tag{4}$$

where $\langle v\rangle = (v_{in} + v_{out})/2$ is an approximation to the average fluid velocity. For a general control volume, the frictional loss due to the line length is given by $\left(\frac{L}{d}\right)f_f$ times the pressure head and that due to a fitting is given by the loss coefficient K times the pressure head. The pressure head in a general control volume is given by $\frac{1}{2}\langle\rho\rangle\langle v\rangle^2$, and the friction factor f_f is calculated using the Haaland expression [5], modified for two-phase flow as in [3]. We note that the LCV is the only line element in the LHe transfer line that is treated specially; it is an equal-percentage-opening type valve with loss coefficient $K_{vs} = 5.0$ m^3/(h bar$^{1/2}$) when fully open. The full model equation for the LCV can be obtained from [6].

2.3. Energy balance for two-phase flow system

The overall energy balance for a control volume is

$$\begin{aligned}\frac{\mathrm{d}E_{tot}}{\mathrm{d}t} &= \rho_{g,in}\alpha_{in}A_{in}v_{in}\left(\mathcal{H}_{g,in}+\frac{1}{2}v_{in}^2+gz_{in}\right)\\ &+\rho_{l,in}(1-\alpha_{in})A_{in}v_{in}\left(\mathcal{H}_{l,in}+\frac{1}{2}v_{in}^2+gz_{in}\right)\\ &-\rho_{g,out}\alpha_{out}A_{out}v_{out}\left(\mathcal{H}_{g,out}+\frac{1}{2}v_{out}^2+gz_{out}\right)\\ &-\rho_{l,out}(1-\alpha_{out})A_{out}v_{out}\left(\mathcal{H}_{l,out}+\frac{1}{2}v_{out}^2+gz_{out}\right)\\ &+\dot{Q}_{ext}-\dot{W},\end{aligned}$$

where E_{tot} is the total energy of the control volume, $\mathcal{H}$ denotes the enthalpy, $\dot{Q}_{ext}$ is the rate of external heat transferred to the system, and $\dot{W}$ is the rate of work done by the system. For a steady-state model, the time derivative term on the left-hand side vanishes, yielding

$$\begin{aligned}0 &= \rho_{g,in}\alpha_{in}A_{in}v_{in}\left(\mathcal{H}_{g,in}+\frac{1}{2}v_{in}^2+gz_{in}\right)\\ &+\rho_{l,in}(1-\alpha_{in})A_{in}v_{in}\left(\mathcal{H}_{l,in}+\frac{1}{2}v_{in}^2+gz_{in}\right)\\ &-\rho_{g,out}\alpha_{out}A_{out}v_{out}\left(\mathcal{H}_{g,out}+\frac{1}{2}v_{out}^2+gz_{out}\right)\\ &-\rho_{l,out}(1-\alpha_{out})A_{out}v_{out}\left(\mathcal{H}_{l,out}+\frac{1}{2}v_{out}^2+gz_{out}\right)\\ &+\dot{Q}_{ext}-\dot{W}.\end{aligned} \tag{5}$$

When there is no work done by the system, $\dot{W}=0$. The term $\dot{Q}_{ext}$ includes radiation from the nitrogen-jacketed pipe enclosing the LHe and GHe lines; see Section 6.1. The lines are also insulated with multiple layers of insulation (MLI) of Aluminized Mylar interleaved with Dexter paper. The Dexter paper reduces conduction, whereas the Aluminized Mylar surface shields the line from external radiation. The heat flux through the MLI is modeled by radiation and conduction fluxes; see [3]. The thermodynamic property models used for calculation of density, internal energy, and enthalpy are the same as in [3].

2.3.1. Work done by the system

In addition to the above equations, the amount of heat that goes into phase change is given by

$$\dot{Q}_{boil} = \zeta \left(\rho_{g,out} \alpha_{out} A_{out} v_{out} - \rho_{g,in} \alpha_{in} A_{in} v_{in} \right),$$

where ζ is the heat of vaporization and the expression in parentheses represents the rate of gas formation r_{boil} given in (1). Because the internal transfer of energy by latent heat of vaporization is not accounted for in the overall energy balance, it can be considered as the work done by the system for interface creation when the gas phase is formed. In fact, we show in Section 6.2 that it is essential to include this term in the place of rate of work done $\dot{W}$ to get good agreement with the measured data.

3. Gas-Phase Flow Model

For the GHe return line, there is no two-phase formation; the void fraction is thus known ($\alpha_{in} = \alpha_{out} = 1$). However, the pressure and temperature are independent variables. Therefore, we still have three unknowns, namely, pressure, temperature, and velocity or gas flow rate that can be obtained from the mass, momentum, and energy balances.

3.1. Mass balance for gas-phase flow system

When considering the overall mass balance on a control volume, there is no generation of mass inside the volume. At steady state, the conservation of mass is given by (2). In terms of gas density ρ_g, area of cross-section A, and homogeneous velocities v, equation (2) becomes

$$\rho_{g,in} A_{in} v_{in} = \rho_{g,out} A_{out} v_{out}. \tag{6}$$

3.2. Momentum balance for gas-phase flow system

The overall momentum balance in a control volume for steady-state conditions is given by (4). The densities are calculated based on the Soave–Redlich–Kwong equation of state for pure gas flow [7]. The GHe return line from the cryostat has a PCV, which is modelled similarly to the LCV on the LHe transfer line. The momentum balance equation for the control valve element is substituted by the pressure drop equation; see [6]. The CRV of the GHe return from cryostat and the PCV on the dewar GHe return line

Location	Loss coefficient for fully open valve (K_{vs})	Valve rangeability (τ)	Valve opening fraction (H)
PCV on GHe return from cryostat	5.0	50	Variable ($0 \rightarrow 1$)
CRV on GHe return from cryostat	5.8	75	1 (fully open)
PCV on GHe return from dewar	1.0	50	Variable ($0 \rightarrow 1$)

Table 1: Control valve parameters.

are modelled similarly. The control valve parameters for the different control valves on the GHe network are given in Table 1.

In addition to the control valves, there is a venturi flow meter on the GHe return line from cryostat that causes a pressure drop. The mass flow rate measured by the venturi meter is correlated to the pressure drop across the meter as follows [2]:

$$\mathcal{F}_v = 0.0481 \Delta P^{\,0.50483}, \tag{7}$$

where the mass flow rate $\mathcal{F}_v$ is given in kg/s and pressure drop ΔP is measured in bars.

3.3. Energy balance for gas-phase flow system

The energy balance for a control volume at steady state is given by

$$\begin{aligned} 0 = {} & \rho_{g,in} A_{in} v_{in} \left(\mathcal{H}_{g,in} + \frac{1}{2} v_{in}^2 + g z_{in} \right) \\ & - \rho_{g,out} A_{out} v_{out} \left(\mathcal{H}_{g,out} + \frac{1}{2} v_{out}^2 + g z_{out} \right) \\ & + \dot{Q}_{ext}. \end{aligned} \tag{8}$$

The rate of heat transferred into the GHe return line $\dot{Q}_{ext}$ comes from heat loading on the vacuum-jacketed (VJ) line or the flexible hose connections [3]. The Soave–Redlich–Kwong equation of state is used for modeling the pressure-volume-temperature relationship [7]. The basic thermodynamic quantity that needs to be calculated is the compressibility of the gas. In practice, if the iteration used to solve the equation of state does not converge to a tolerance of 1×10^{-6} for compressibility of the gas, the thermodynamic property models described in [3] are used.

4. Cryostat Model

The dynamic model of the cryostat is based on the differential equations describing change of gas mass, liquid mass, volume of liquid, and pressure inside the cryostat, as derived in [1]. The final equations used in the present simulation are reproduced here for convenience:

$$\frac{\mathrm{d}m_l}{\mathrm{d}t} = \mathcal{F}_{l,in} - \mathcal{F}_{l,out} - r_{boil}, \tag{9}$$

$$\frac{\mathrm{d}P_c}{\mathrm{d}t} = \frac{a_1}{a_2} + r_{boil}\left(\frac{u_l - u_g}{a_2}\right), \tag{10}$$

where r_{boil} is the rate of boiling of LHe in the cryostat given by

$$r_{boil} = \frac{-\frac{a_1}{a_2}\left(a_3 + 0.0585\, a_4\, m_l\, \phi\, P_c^{-0.748}\right) + a_4\left[\frac{V_g}{m_g}\left(\mathcal{F}_{g,out} - \mathcal{F}_{g,in}\right) + a_5\left(\mathcal{F}_{l,out} - \mathcal{F}_{l,in}\right)\right]}{\frac{u_l - u_g}{a_2}\left(a_3 + 0.0585\, a_4\, m_l\, \phi\, P_c^{-0.748}\right) + a_4\left(\frac{V_g}{m_g} - a_5\right)},$$

where

$$\begin{aligned}
a_1 &= \dot{Q}_c + \mathcal{F}_{l,in}\left(h_{l,in} - u_{l,in}\right) + \mathcal{F}_{g,in}\left(h_{g,in} - u_{g,in}\right) \\
&\quad - \mathcal{F}_{l,out}\left(h_{l,out} - u_{l,out}\right) - \mathcal{F}_{g,out}\left(h_{g,out} - u_{g,out}\right), \\
a_2 &= 0.0585\left(m_l C_{v,l} + m_g C_{v,g}\right) P_c^{-0.748}, \\
a_3 &= 0.0585 P_c^{-0.748} - \frac{\left(16.444 \times 10^{-6} P_c + 0.4967\right) V_g}{R m_g}, \\
a_4 &= \frac{\left(8.222 \times 10^{-6} P_c^2 + 0.4967 P_c\right)}{R m_g}, \\
a_5 &= 0.232 \phi P_c^{0.252} + \psi,
\end{aligned}$$

and P_c is the pressure inside the cryostat, m_l and m_g are the masses of liquid and gaseous helium, V_l and V_g are the volumes of liquid and gaseous helium, $\mathcal{F}_{l,in}$ and $\mathcal{F}_{l,out}$ are the mass flow rates of LHe into and out of the cryostat, $\mathcal{F}_{g,in}$ and $\mathcal{F}_{g,out}$ are the mass flow rates of GHe into and out of the cryostat, respectively, and R is the specific gas constant for helium. The specific enthalpy and internal energy of the streams are represented by h and u with appropriate subscripts. The gas exiting the cryostat is assumed to have the same thermodynamic properties as the gas in the cryostat. The

internal energy and enthalpy for LHe and GHe are calculated based on the NIST database correlations presented in [3]. The constants $\phi = 0.0017612$ and $\psi = 0.0004873$ for the linear correlation of the specific volume (a_5) are based on the NIST database [2] as a function of temperature. The cryostat is assumed to be operating in thermal equilibrium at all times. The constant volume heat capacities are $C_{v,l} = 2584$ J/(kg K) and $C_{v,g} = 3201$ J/(kg K) for liquid and gas, respectively. The rate of heat input into the cryostat is $\dot{Q}_c$ consists of three portions, namely, the rates of heat input from RF cavity ($\dot{Q}_{RF}$), the heating resistor ($\dot{Q}_H$), and the static heat loading from the surroundings ($\dot{Q}_s$), and is calculated according to the procedure described in [2]. The present method using the control-volume approach gives the following static-heat-loading correlation as a function of various measured values of heater power inputs:

$$\dot{Q}_s = -0.27874\dot{Q}_H + 54.754. \tag{11}$$

4.1. Controller model

The normal pressure in the cryostat is to be maintained within ±1 mbar for consistent operation of the RF Cavity. Both the level of the LHe and pressure of the GHe are regulated by PI controllers. The control valve lift at time level i is calculated as

$$H(i) = \mathcal{K}_p \left(\epsilon(i) + \frac{1}{T_I} \sum_{j=1}^{i} \epsilon(j)\Delta t \right), \tag{12}$$

where the error is calculated as $\epsilon(i)$ = (Set value – Measured value) for mode-1 operation (positive mode) and $\epsilon(i)$ = (Measured value – Set value) for mode-2 operation (negative mode). For the integral controller, the summation is from the start of operation ($j = 1$) to current time level ($j = i$) after i time steps of size Δt. Also, $\mathcal{K}_p$ is the proportional gain of the controller, and T_I is the time constant for the integral controller. The level controller operates in mode 1, and the pressure controller operates in mode 2. The controller settings normally used are given in Table 2.

4.2. Cryostat and Level Controller Interaction

The operation of the pressure controller is based on the cryostat pressure P_c obtained by solving (10). However, (9) provides the mass of LHe. Hence, the mass must be converted to the equivalent level of liquid in the cryostat for

Controller	Set Value	$\mathcal{K}_p$	T_I
LCV on LHe	70–75%	10%/%	100 s
PCV on GHe	1.22 bars	20%/bar	50 s
FCV on waveguide stream	25 L/min	2%/(L/min)	10 s

Table 2: Controller parameters.

operation of the LCV. The mass of LHe is readily converted to volume of LHe in the cryostat using the specific volume correlation obtained from the NIST database; see Section 4. The volume-to-level and level-to-volume conversions are challenging due to the presence of equipment inside the cryostat. In order to correlate the level of liquid in the cryostat to the volume of liquid, the cryostat is filled in level increments of 1 cm and the volume of liquid required is tabulated [2, Ch. 4]. Determination of the actual level L_A in the cryostat is further complicated due to the shape of the level-sensing element. The correlation between L_A and the indicated level L_I is derived in [2, Ch. 7]:

$$L_A = \frac{100}{116}\left[57.722 - 74.487 \sin\left(0.8866 - \frac{1.676 L_I}{74.487}\right)\right]. \tag{13}$$

Using the tabulated data, the cumulative volume is calculated by summing the volume increments for every 1 cm of level increase up to a given L_A, with care being taken to correct for fractional values. The reverse process gives L_I for a given volume of liquid. When it is full, the volume of liquid inside the cryostat is 502 L.

5. Numerical Methods

In this section, we present the details of the control-volume approach for simulating the LHe transfer line and the GHe return line and couple it to the dynamic simulation of the cryostat.

5.1. Control-volume specification

The results of lumped system simulation of the LHe transfer line and GHe return network presented in Section 6 are based on points specified along the length of the pipe. The locations of the points used for the simulations are presented in Table 3 for the LHe transfer line. A similar table of points

can be generated for GHe return network; see [8] for details. Depending on the accuracy of the simulation required and the details of the known pipe elements, any number of points can be specified. Typically points are taken at the end of a straight pipe or on either side of pipe fittings such as elbows, valves, etc. For this study, it was sufficient to compute 36 control volumes to get accurate results for the LHe transfer line. It was also the minimum required to capture all the features in the line. The line segment from the T-junction to the compressor suction is treated as a single control volume (with end points at the T-junction outlet and the compressor suction inlet). This line segment represents the heat exchanger network. The detailed specifications of the exchangers and the pipe fittings are not known. However, an effective loss coefficient (K_{eff}) for this network is estimated using known mass flow rates as per the procedure described in Section 5.3 and used for all subsequent simulations. The equations for mass balance (3), momentum balance (4), and energy balance (5) are solved for each of the control volumes defined between any two points using the `fsolve` routine in MATLAB.

5.2. Solution for the LHe transfer line

For the LHe transfer line, the three variables at any point are the pressure, velocity, and void fraction. By assuming saturated fluid conditions throughout the pipe, we can eliminate temperature as a degree of freedom. For the first control volume, the inlet void fraction of the fluid stream is assumed to be zero; i.e., the liquid is saturated. The pressure at the inlet of the pipe is known; it is equal to dewar operating pressure. We then need to compute the velocities at the inlet and outlet as well the void fraction at the outlet. The pressure at the outlet of the first control volume is not known. However, the outlet pressure of the final control volume is known; it is equal to the cryostat pressure. If there are n control volumes, we can write $3n$ equations. At the first point, there is 1 unknown, at the last point there are 2 unknowns, and at all $n-1$ intermediate points, there are 3 unknowns, thus adding up to $3n$ variables.

The boundary values and the corresponding thermodynamic properties for LHe transfer line are known or estimated [9] and given in Table 4.

5.3. Solution for the GHe network

The GHe network has three segments and the T-junction. There are three terminals, namely, the cryostat, the dewar, and the compressor suction; see

Point no.	Location along the pipe (in m)	Elevation (in m)	Length of line segment (in m)	Diameter of line (in m)	Loss Coefficient (K_i)
1	0	0	0	0.009398	0
2	0	0	0	0.009398	1
3	1.75	1.75	1.75	0.009398	0
4	4.29	3.546	2.54	0.009398	0
5	6.37	5.626	2.08	0.009398	0
6	6.37	5.626	0	0.009398	2
7	13.76	5.626	7.39	0.009398	0
8	13.76	5.626	0	0.009398	0.5
9	28.12	5.626	14.36	0.009398	0
10	28.12	5.626	0	0.009398	0.5
11	34.46	5.626	6.34	0.009398	0
12	34.46	5.626	0	0.009398	0.4
13	35.099	5.066	0.639	0.009398	0
14	35.25	5.066	0.151	0.009398	0
15	35.25	5.066	0	0.009398	0.4
16	38.12	5.066	2.87	0.009398	0
17	38.12	5.066	0	0.009398	0.2
18	40.71	5.066	2.59	0.009398	0
19	40.71	5.066	0	0.009398	0.4
20	41.497	5.726	0.787	0.009398	0
21	41.65	5.726	0.153	0.009398	0
22	41.65	5.726	0	0.009398	0.4
23	47.89	5.726	6.24	0.009398	0
24	47.89	5.726	0	0.009398	0.1
25	52.61	5.726	4.72	0.009398	0
26	52.61	5.726	0	0.009398	0.5
27	52.858	6.006	0.248	0.009398	0
28	53.35	6.006	0.492	0.009398	0
29	53.35	6.006	0	0.009398	0.15
30	55.7	6.006	2.35	0.009398	0
31	55.7	6.006	0	0.009398	2
32	55.898	5.306	0.198	0.009398	0
33	57	4.204	1.102	0.009398	0
34	57	4.204	0	0.009398	-1
35	60.2	4.204	3.2	0.009398	0
36	60.2	4.204	0	0.009398	2
37	60.3	0.904	0.1	0.009398	0

Table 3: Points chosen for the LHe transfer line simulation.

Property	Inlet	Outlet
Pressure (P, in bars)	1.37	1.22
Temperature ($T = T_{sat}$, in K)	4.5682	4.4345
Height (z, in m)	0.0	0.105
Diameter (d, in m)	0.009398	0.009398
Liquid		
Enthalpy (h_l, in J/kg)	2037.2	1173.6
Internal Energy (u_l, in J/kg)	866.94	160.13
Density (ρ_l, in kg/m^3)	117.06	120.38
Gas		
Enthalpy (h_g, in J/kg)	20394	20619
Internal Energy (u_g, in J/kg)	14509	14640
Density (ρ_g, in kg/m^3)	23.278	20.407

Table 4: Boundary values for simulation and corresponding thermodynamic properties.

Figure 1. The pressures and temperatures at these points are known. However, the mass flow rates are dependent on the valve openings. Accordingly, the solution procedure consists of the following steps:

1. For the GHe return line from the cryostat, the pressure and temperature at the inlet, i.e., the outlet of the cryostat, are known; they are taken to be the same as the cryostat pressure ($P_{in} = P_c$) and temperature ($T_{in} = T_c$). The pressure ($P_{out} = P_T$) and temperature ($T_{out} = T_{T,c}$) at T-junction and the velocities v_{in} and v_{out} are unknown. Thus, there are four variables. However, there are only three equations, viz., mass balance (6), momentum balance (4), and energy balance (8). The procedure is started with an initial guess of the mass flow rate from the cryostat $\mathcal{F}_c$, yielding v_{in} for a given PCV opening. The (potentially unconverged) values of P_T, $T_{T,c}$, and v_{out} can then be calculated using the three equations.

2. Using the pressure at the T-junction (P_T) calculated above, the GHe return line from dewar can be solved for the velocities and temperature at the T-junction using the same equations, viz., (6), (4), and (8). The temperatures and velocities of GHe return streams from cryostat and dewar are generally different. Let $T_{T,d}$ be the temperature of the stream from the dewar and $\mathcal{F}_d$ be the mass flow rate.

3. The mass balance gives the total mass flow rate to the compressors:

$$\mathcal{F}_{tot} = \mathcal{F}_d + \mathcal{F}_c.$$

4. The energy balance at the T-junction gives the temperature of the mixed stream as

$$T_T = (\mathcal{F}_c T_{T,c} + \mathcal{F}_d T_{T,d})/\mathcal{F}_{tot}.$$

5. The pressure (P_{cp}) and temperature (T_{cp}) at the compressor suction are known. Given the loss coefficient across the heat exchanger network (K_{eff}), the velocity at the compressor suction can be calculated using the momentum balance equation (4). This value can then be used for updating the mass flow rate ($\mathcal{F}_c$) in the GHe return stream from cryostat in the first step.

In order to estimate K_{eff}, the above calculations are performed with known values of gas mass flow rates from cryostat measured by the venturi meter (7). A sample of the measured data is given in Table 7. The PCV on the dewar is open 80% at all times, and the CRV is fully open. Using these data, a K_{eff} value of approximately 54 is obtained. This value is used for subsequent simulations where the mass flow rate from cryostat is unknown. This is the case in the following dynamic simulation, where the cryostat valve is dynamically operated based on the pressure in the cryostat.

5.4. Dynamic simulation of the cryostat

The cryostat model is a dynamic model based on ordinary differential equations of the form $\frac{\mathrm{d}y}{\mathrm{d}t} = f(t, y)$ that are discretized in time by the first-order explicit forward Euler scheme,

$$\frac{y_i - y_{i-1}}{\mathrm{dt}} = f(t_{i-1}, y_{i-1}), \tag{14}$$

by the first-order implicit backward Euler scheme,

$$\frac{y_i - y_{i-1}}{\mathrm{dt}} = f(t_i, y_i), \tag{15}$$

or by the second-order implicit Crank–Nicolson scheme

$$\frac{y_i - y_{i-1}}{\mathrm{dt}} = \frac{1}{2}\left(f(t_i, y_i) + f(t_{i-1}, y_{i-1})\right). \tag{16}$$

The time step size has been denoted by dt for future reference. The time step dt is assumed to be sufficiently small but not infinitesimal. In our simulations, we have taken dt $= \Delta t$ from (12), but this is not a requirement.

In order to simulate the cryostat dynamics, the following iteration for any time level i is followed:

- Given the pressure in the cryostat and the dewar at time level i, equations (3), (4), and (5) for the LHe transfer line are solved for the liquid and gas flow rates into the cryostat.

- Given the pressures in the cryostat, the dewar, and at the compressor suction at time level i, the equations for the GHe return network are solved for the gas flow rate out of the cryostat following the procedure in Section 5.3. Note that a small constant stream of gas is drawn to cool the waveguide attached to the cryostat.

- Using the flow rates of liquid and gas into and out of the cryostat along with the heater power input, the change in mass of LHe inside the cryostat (9) can be calculated. Using the procedures for volume-to-level conversion and level-to-volume conversion in [2], the level of LHe can be estimated. Using the differential equation for pressure (10), the cryostat pressure at the next time level $i + 1$ can be determined.

- The updated pressure and level in the cryostat at time level $i + 1$ are used for calculating the error terms $\epsilon(i)$ at time level i in equation (12). The pressure controller on the cryostat is mode-2 operation; i.e., if the pressure is higher than the set pressure, the error is positive and the PCV must open to relieve some of the gas in the cryostat. The level controller on the cryostat is in mode-1 operation; i.e., if the level is lower than the set level, the error is positive and LCV must open to allow flow into the cryostat. After the correction, the valve position at the time level $i + 1$ is known.

- Using the updated valve positions and pressure in the cryostat, the procedure can be repeated for the next time level.

For the explicit scheme, the flow rates in the above iteration scheme are determined based on the current time level values of pressure. For the implicit scheme, the flows rates are updated based on the predicted pressure in the cryostat, and these updated flow rates are then used to correct the

pressure and the level in the cryostat before making changes to the valve positions of the pressure and level control valves. Alternatively, the values of the flow rates obtained at current and predicted values of pressure can be averaged to obtain a corrected pressure and level in the cryostat that can then be used for updating the valve positions. This leads to the second-order implicit Crank–Nicolson scheme.

6. Simulation Results

In this section, we present the validation of liquid and gas flow rates from the LHe transfer line into the cryostat. This is a critical test for the accuracy of the model and the numerical methods. The second validation case presented is the dynamic operation of the cryostat along with the controllers in response to heater power step-input changes. This test assesses the accuracy of not only the LHe transfer line calculations but also the GHe return network along with the cryostat and controller models. The dynamic one-dimensional homogeneous model from [1] is used for a comparison of the results.

6.1. External heat transfer

The rate of heat transfer by conduction and radiation according to the heat network equation in [8] is evaluated using non-linear equations solver `fsolve` in MATLAB. The output from the program is tabulated in Table 5 for the LHe transfer line and the GHe return network.

Presently the simulation uses 5 layers of Aluminized Mylar Insulation on the LHe line inside the flexible line from the dewar to the VJ line and the flexible line from the VJ line to the cryostat. The same number of layers is assumed for the other flexible lines. The LHe and GHe lines inside the VJ line have 20 layers each.

In addition to the heat transferred by radiation from the jacket pipe and conduction through the MLI, there is also conduction from the jacket pipe through the spacer material. The estimate of this rate of heat transferred is given in [2] as 1.005 W into the LHe transfer line and 2.01 W into the GHe return line from the cryostat. The heat transferred through the spacers is distributed equally among the 32 spacers.

The control valve stem is also a source of heat load into the LHe line and is estimated to be 0.59 W for the LCV. The same value is used for the PCV on the GHe return line from the cryostat, and the CRV puts in an additional

Line Section	MLI Outer Layer Temperature	MLI Outer Layer Emissivity	Radiative Resistance ($1/m^2$)	Rate of external heat transferred per unit length (W/m)	Rate of external heat input in section (W)
LHe transfer line					
Dewar Flex Line:	228.4	0.0211	341.69	0.31073	0.789
Main VJ Line - LHe:	9.7	0.0122	16.00	0.00241	0.125
Cryostat Flex Line:	223.0	0.0209	250.69	0.43041	1.132
GHe return line					
Cryostat flex line:	220.5	0.0208	200.23	0.55087	1.449
Main VJ Line - GHe:	8.9	0.0122	11.71	0.00330	0.170
Coldbox Flex Line:	223.7	0.0209	184.48	0.43192	1.529
Dewar Return Line:	279.6	0.0231	68.87	0.27304	1.119

Table 5: The rate of external heat transferred into various sections by radiation and conduction through MLI surface.

0.47 W into this line. The heat loading through the valve stem of the PCV on the GHe return from the dewar is 0.47 W. The heat input through the control valve is used when solving for the control volume containing the control valve.

The total heat loading on the LHe transfer line is estimated as 3.59 W, on the GHe return line from the cryostat as 6.15 W, and on the GHe return line from the dewar as 1.59 W. These values are comparable to those in [1].

6.2. The liquid flow rate

The liquid flow rate calculated is plotted for various control valve lift positions H from a value of 0.0 for fully closed to 1.0 for fully open. Figure 2 compares the present program output to that of the one-dimensional homogeneous model [2]. It is observed that the results obtained by incorporating

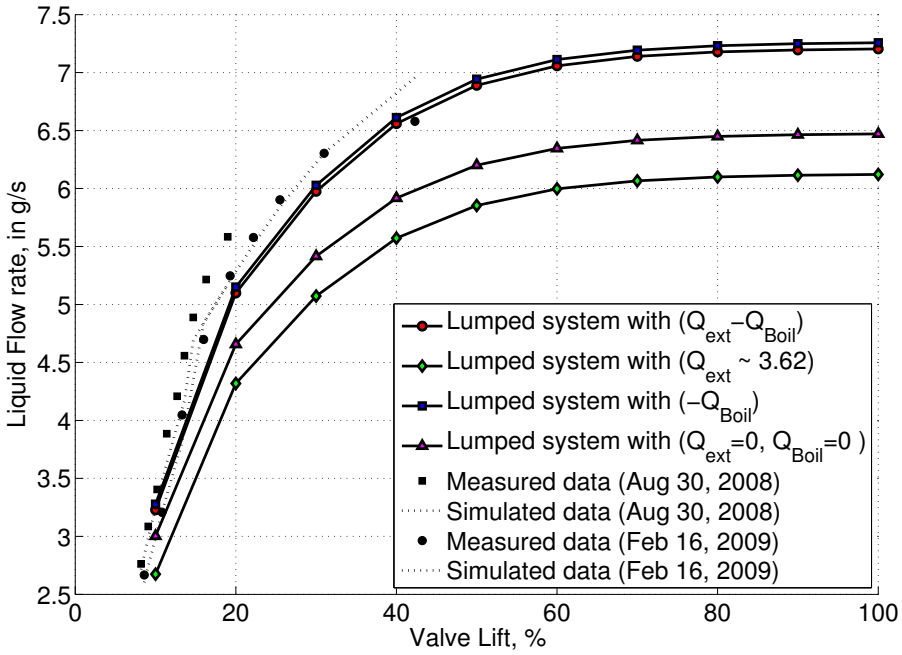

Figure 2: Liquid flow rates into the cryostat for various valve lift positions.

only the $\dot{Q}_{boil}$ term in the energy balance equation yields the best agreement with the measured data available from the process. The predicted liquid flow rate is dramatically affected by the absence of the $\dot{Q}_{boil}$ boil. In contrast, the presence of the $\dot{Q}_{ext}$ term has little effect.

6.2.1. Sensitivity analysis: control valve chattering

Changes in the liquid flow rate due to changes in the control valve opening are investigated for valve openings of 1% around values of $H = 0.1$ to $H = 0.9$. The results are presented in Table 6. It is clear that as the valve opens,

Mean Valve Opening (H)	Mean Mass Liquid Flow Rate ($\mathcal{F}_l$, in g/s)	Change in Liquid Flow Rate
0.10	3.23	26.09
0.20	5.10	10.01
0.30	5.98	7.34
0.40	6.56	4.43
0.50	6.89	2.35
0.60	7.06	1.15
0.70	7.14	0.55
0.80	7.18	0.25
0.90	7.20	0.12

Table 6: Sensitivity of liquid flow rate on 1% change in valve opening.

the control on the liquid flow rate decreases; therefore the sensitivity of the liquid flow rate on the valve position also decreases.

6.3. Heater step-input validation

The data from the heater step test are given in Table 7. Only the heater power input is required as input to the simulation along with the initial conditions. The cryostat pressure is regulated at 1.22 bars, and the level is regulated at 75%.

6.3.1. Comparison of numerical schemes

Due to the high sensitivity of the LCV at low openings, the explicit forward Euler scheme suffers from numerical oscillations and becomes unstable. In Figure 3, we compare the explicit forward Euler and implicit backward Euler schemes for the same time step size. These plots illustrate the superior stability of implicit backward Euler scheme. In the light of this, we use only the implicit schemes for the remaining simulations.

In Figures 4 and 5, we compare the performance of the first-order implicit backward Euler scheme with the second-order implicit Crank–Nicolson scheme for the calculation of the LCV and PCV positions, respectively. Both

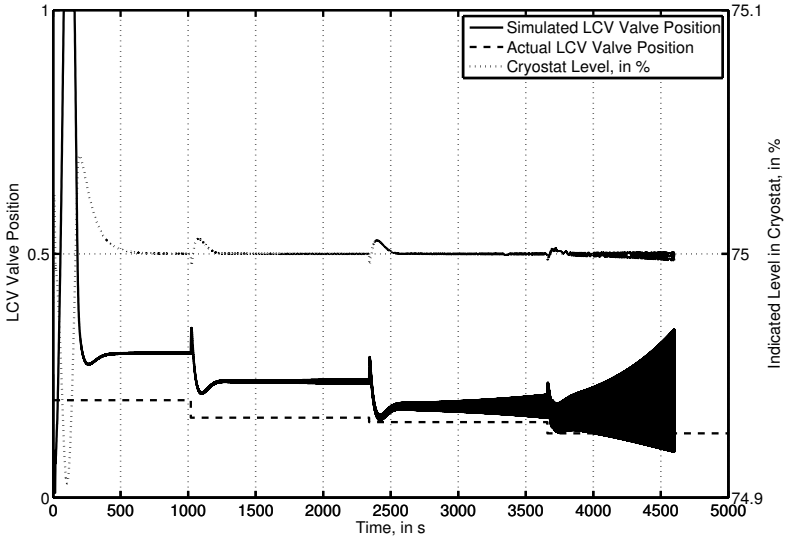

(a) Explicit forward Euler scheme for dt = 0.50 s.

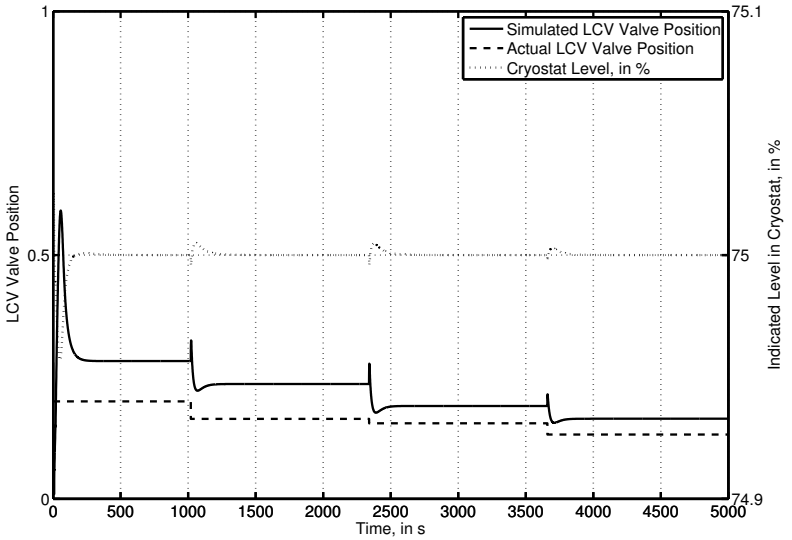

(b) Implicit backward Euler scheme for dt = 0.50 s.

Figure 3: Comparison of explicit forward Euler scheme and implicit backward Euler scheme at dt = 0.5 s for level control, illustrating the stability of the implicit scheme.

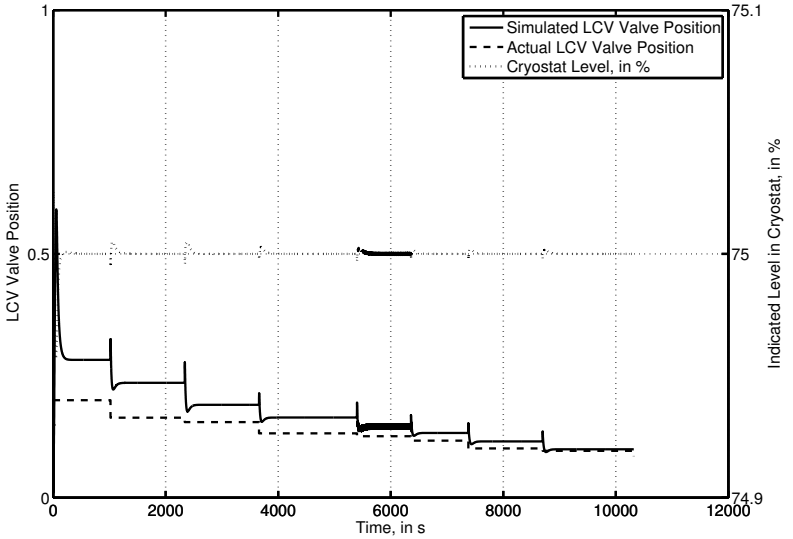

(a) First-order implicit backward Euler scheme for dt = 0.50 s.

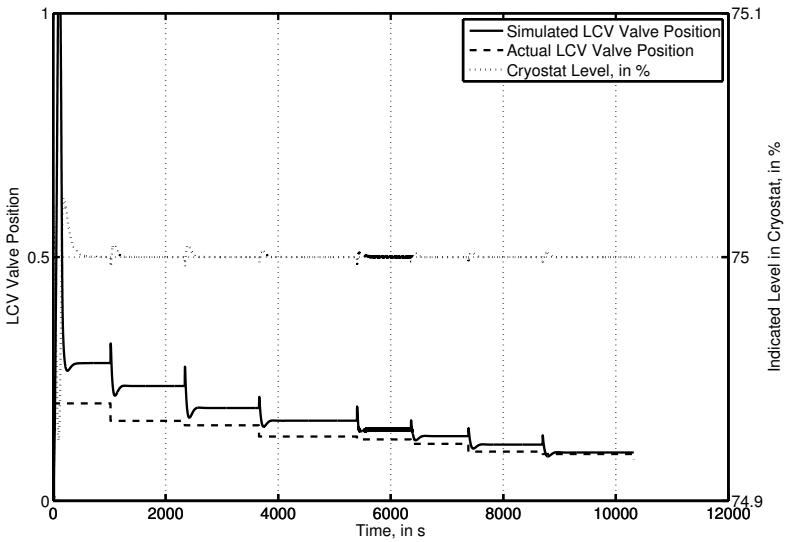

(b) Second-order implicit Crank–Nicolson scheme for dt = 0.50 s.

Figure 4: Comparison of the first-order implicit backward Euler scheme and the second-order implicit Crank–Nicolson scheme at dt = 0.5 s for level control.

Time	Heater Power	Venturi Mass Flow (kg/s)	LHe Supply Valve Position (% open)	GHe Return Valve Position (% open)
0.00	80.25	5.72×10^{-3}	19.0	41.3
1020.00	69.50	5.34×10^{-3}	16.3	38.2
2340.00	57.78	5.01×10^{-3}	14.7	34.9
3660.00	50.49	4.68×10^{-3}	13.6	32.4
5400.00	40.89	4.33×10^{-3}	12.7	30.4
6360.00	30.89	4.00×10^{-3}	11.4	28.0
7380.00	20.47	3.52×10^{-3}	10.2	24.6
8700.00	9.62	3.19×10^{-3}	9.1	21.6
10320.00	0.00	2.87×10^{-3}	8.2	19.3

Table 7: Data for cryostat heater step test.

schemes accurately predict the pressure in the cryostat as well as the valve position in controlling the pressure at a constant value. However, the second-order scheme suffers from an initial transient overshoot because it is slightly less stable.

In Figure 6, the gas mass flow rate calculations from the dynamic simulation of cryostat using both first-order and second-order implicit methods (shown with bold lines) are compared to the results of the simulation based on the one-dimensional homogeneous model using a linear correlation for static heat loading as a function of heater power input (shown with dotted lines) and a constant value of static heat loading $\dot{Q}_s = 37.2$ W (shown with dashed lines). The linear correlation for static heat loading used with the present control-volume method is obtained using the same procedure that is described in [2]; however the calculations are performed using the numerical methods described in Section 5. The circles indicate the times at which a change in heater power input is implemented. The squares represent the measured data obtained by running the cryostat in maintenance mode with different heater power inputs. The times and heater power input steps along with the gas mass flow rate and valve positions are noted in Table 7. Both first-order and second-order implicit methods give better results for the gas flow rate as compared to previously used methods.

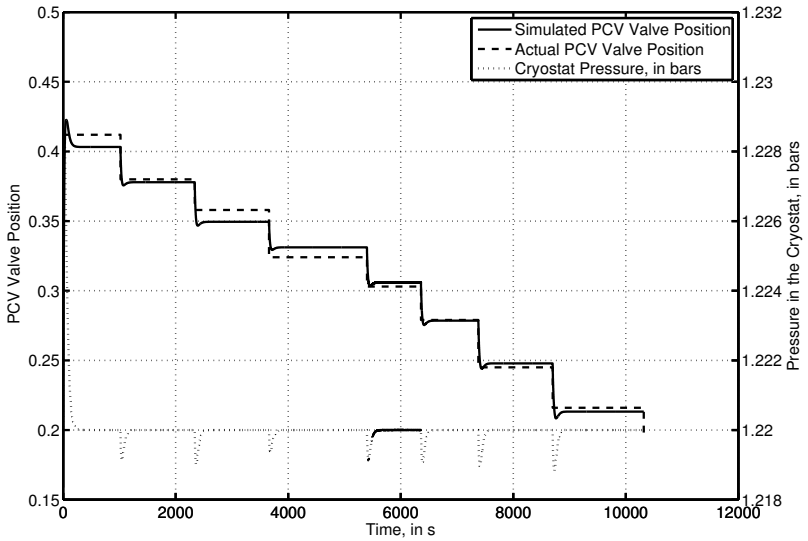

(a) First-order implicit backward Euler scheme for dt = 0.50 s.

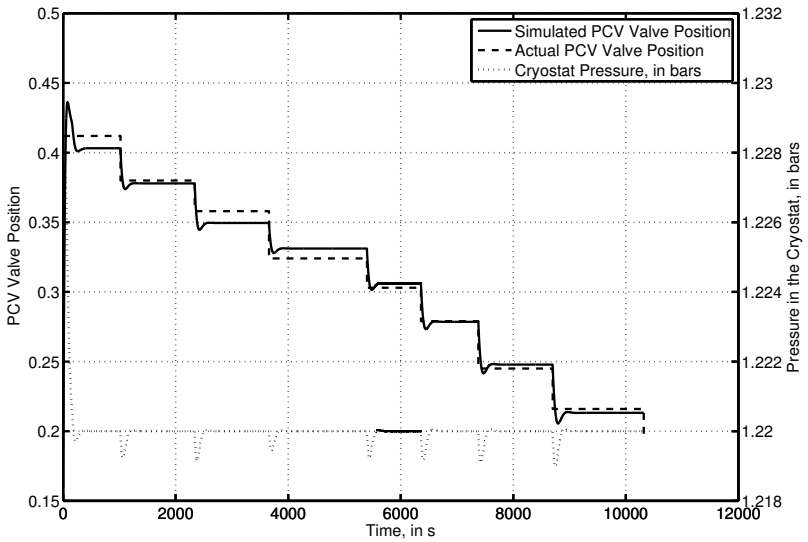

(b) Second-order implicit Crank–Nicolson scheme for dt = 0.50 s.

Figure 5: Comparison of the first-order implicit backward Euler scheme and the second-order implicit Crank–Nicolson scheme at dt = 0.5 s for pressure control.

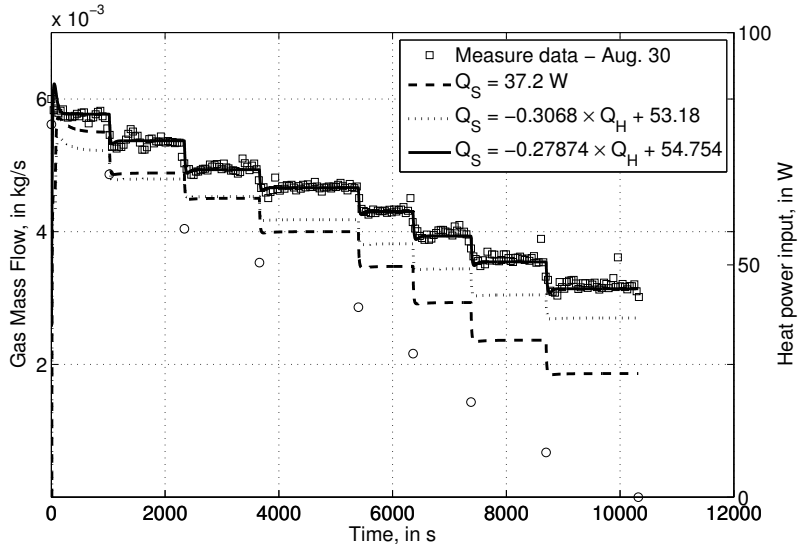

(a) First-order implicit backward Euler scheme for dt = 0.50 s.

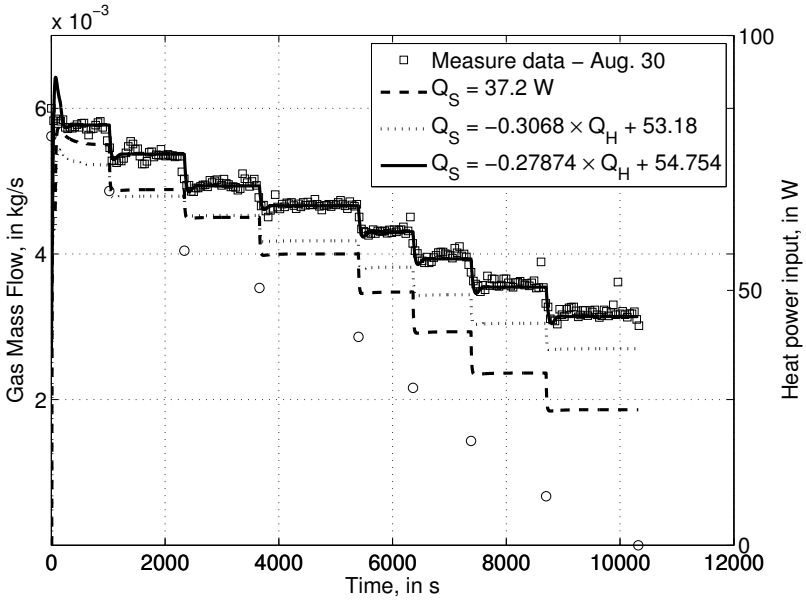

(b) Second-order implicit Crank–Nicolson scheme for dt = 0.50 s.

Figure 6: Comparison of first- and second-order implicit schemes for cryostat simulation with time step size of dt = 0.5 s.

6.4. Performance of the code

For steady-state simulations of the LHe transfer line, the algorithm in [1] used transient calculations to converge to a steady-state solution, requiring approximately 200 to 300 s of wall clock time, depending on the valve opening. If only steady-state solutions are of interest, i.e., final liquid and gas flow rates into the cryostat, then the approach presented here gives equivalent results in approximately 5 s for a speedup factor of between 40 and 60. These timings are estimates obtained from simulations run on a machine with dual 2 GHz PowerPC G5 with memory of 1 GB DDR SDRAM. The codes are based on MATLAB 7.5 (R2007b) and run under the MAC OS X Version 10.5.8 operating system. Further benchmarking of the code for dynamic simulations will be reported elsewhere.

7. Conclusions

The model [1] for the cryogenic system at the CLS is based on a one-dimensional, homogeneous model of two-phase helium flow. This paper describes a mathematical model for the same system and the development of a more accurate, efficient, and flexible computational method based on a control-volume approach. The faster computation compared to the one-dimensional homogeneous code and the two validations cases, viz., the liquid flow rate calculations for different valve openings and the gas mass flow rate for heater power step test, demonstrate the accuracy of the model and performance of the computational method. The proposed approach can simulate varying process line lengths and hence can be used for calculations prior to any process modifications. Furthermore, with this approach new process equipment can be easily added.

An investigation of the physical meaning of the additional heat term $\dot{Q}_{boil}$ that better predicts measured data is desirable. A heat of boiling term was proposed in [2] and included in the overall energy balance equation for two-phase flow. In the present model, the term is interpreted as the additional work done by the system. We hypothesize that a part of the total energy of the system may be used in creating additional interfacial boundaries. When phase change occurs, gas bubbles are formed either due to nucleation by cavitation (i.e., flashing of liquid due to reduction in pressure) or due to nucleation by boiling (i.e., flashing of liquid due to increase in temperature). After nucleation, the bubbles grow as helium transforms from the liquid phase to the gas phase. There is further work done by turbulence in the

breaking of bubbles. The homogeneous model may not be sufficient to capture the physics of the nucleation; hence a more thorough model based on heterogeneous flow may be required to capture the interfacial physics.

Acknowledgement

The authors would like to thank C. Regier for helpful discussions and for supplying the measured data. We also thank J. Boisvert and C. Marsh for computer support. This work was funded jointly by Mitacs and the CLS (through a Mitacs Accelerate Internship) and NSERC.

Reference

[1] C. Regier, J. Pieper, E. Matias, Dynamic modeling of a liquid helium cryostat at the Canadian Light Source, Cryogenics 50 (2010) 118–125.

[2] C. N. Regier, Dynamic modeling of a cryogenic system at the Canadian Light Source, Ph.D. thesis, University of Calgary, Calgary, AB, Canada (2009).

[3] C. Regier, J. Pieper, E. Matias, A dynamic model of a liquid helium transfer line at the Canadian Light Source, Cryogenics 51 (2011) 1–15.

[4] R. B. Bird, W. E. Stewart, E. N. Lightfoot, Transport Phenomena, John Wiley and Sons, New York., 1960.

[5] F. White, Fluid Mechanics, McGraw Hill Inc., New York., 1994.

[6] Control valve characteristics., Available at: Spirax Sarco Ltd. (2010).

[7] J. M. Smith, H. C. Van Ness, M. M. Abbott, Introduction to Chemical Engineering Thermodynamics, McGraw-Hill Companies, Inc., 1996.

[8] C. Veeramani, R. J. Spiteri, Modeling and simulation of the CLS cryogenic system, Tech. Rep. 2010-003, Deparment of Computer Science, University of Saskatchewan (2010).

[9] E. Lemmon, M. McLinden, D. Friend, Thermophysical properties of fluid systems, NIST Chemistry Webbook, NIST Standard Reference Database (69), available at: NIST Webbook.